Spectrochimica Acta A 58,1 (2002) 1-15.

Influence of dehydration effects on the optical spectra of $H_4PVMo_{11}O_{40}$ in the visible and near infrared range: Intra- and intercenter optical transitions in the V-Mo -cluster

S. Klokishner[1)], J. Melsheimer[2)], R. Ahmad[2)], F.C. Jentoft[2)], G. Mestl[2)], and R. Schlögl[2)]

[1)] **State University of Moldova, Mateevich Str. 60, 2009 Kishinev , Moldova.**

[2)] **Fritz-Haber-Institut der Max-Planck-Gesellschaft, Faradayweg 4-6, 14195 Berlin, Germany**

Abstract

UV/Vis/NIR diffuse reflectance spectra of heteropoly acids of the type of $H_4PVMo_{11}O_{40} \cdot x\ H_2O$ were recorded with improved spectroscopic equipment for different times on helium stream at room temperature. A broad asymmetric absorption band with a maximum at 740-780 nm in the visible (Vis) range and a shoulder at 900-1000 nm in the near infrared (NIR) range is identified. With increasing time on stream the intensity of this band grows appreciably: simultaneously, the water peaks at 1430 nm and 1925 nm decrease.

Focussing on a single mixed-valence $V^{4+} - Mo^{6+}$ -cluster, a model is suggested for the description of the experimental results. The model takes into account electron transfer, low symmetry crystal fields and vibronic interaction. The absorption band shape calculation is performed within the semiclassical limits. The band shape is shown to be determined both by the optical d-d transitions in V^{4+} and Mo^{5+} and the intervalence $V^{4+} - Mo^{6+}$ optical transition. Appreciable changes in the band intensity are attributed to the increase of the electron transfer parameter due to water loss. Quite good agreement with the experiment was found for a reasonable set of transfer and vibronic parameters.

Author Keywords: UV/Vis/NIR diffuse reflectance spectroscopy; Apparent Absorption; Charge transfer band; Optical d-d transitions

1. Introduction

Intensive studies have been made of vanadomolybdophosphate heteropoly acids $H_{3+n}\,PV_nMo_{12-n}O_{40}$ (n = 0-3) (HPA), which have attracted wide scientific interest as catalysts. Heteropolyacids are composed of primary, secondary and tertiary structures. The primary structures represent the main building blocks of the HPA. These blocks have the form of Keggin units [1]. In the Keggin unit, four triads of M_3O_{13} ions can be distinguished where M is a transition metal ion. In each triad the MO_6 octahedra are joined with two neighbours along an edge and with two octahedra from neighbouring triads through an apex. The three-dimensional arrangements of the Keggin polyanions, cations and other components of the HPA are regarded as the secondary structures. Tertiary structures can be observed when heavy alkali salts are formed [2]. Meanwhile in the mixed HPA compounds the Mo and V ions are distributed randomly. Moreover, depending on the manner of compound preparation, the vanadium ions can be located inside the primary (oxoanion) and/or the secondary structure [3,4]. The vast experimental material also shows that heteropoly acids crystallize with a large number of water molecules : crystal and constitutional water. Under the action of an inert gas stream or when the temperature rises, the water can be removed. Two temperature regions of water loss exist, corresponding to two types of water. The widths of these regions and the starting points depend on the compound structure [5]. The characteristics and attributes of HPA are exhibited

clearly in the UV/Vis/NIR spectra. UV/Vis/NIR reflectance spectroscopy allows us to follow in situ the transformations of the HPA catalysts during thermal treatment, action of an inert gas and the catalytic reaction [6]. Meanwhile, to our knowledge no attempts at a theoretical analysis of the optical spectra of the HPA have been undertaken up until now. In the present paper the UV/Vis/NIR diffuse reflectance spectra of $H_4PVMo_{11}O_{40} \cdot x\ H_2O$ compound for different times on helium stream will be studied experimentally and theoretically.

2. Experimental details and results

A Perkin Elmer Lambda 9 spectrometer and a flow-through microreactor were used for in situ UV/Vis/NIR diffuse reflectance spectroscopy. The spectrometer is equipped with an integrating sphere together with an appropriate microreactor.

All spectroscopic measurements were carried out sequentially with spectralon as reference material. The apparent absorption was evaluated from the diffuse reflectance data using the formula $1\text{-}R_{mixture}/R_{SiO2}$. Mixtures of $H_4PVMo_{11}O_{40} \cdot x\ H_2O$ and quartz (Hereaus) were made by grinding in the ratio 1 : 10.

The compound $H_4PVMo_{11}O_{40} \cdot x\ H_2O$ was prepared from stoichiometric mixtures of metal oxides (MoO_3, V_2O_5) and phosphoric acid in water. The details of the spectrometer equipment are described in [7] and that of the synthesis in [8]. We arrived at the following numbering of the the UV/Vis/NIR diffuse reflec-

tance spectra : 1, 2, 3, 4, 5, 6 and 7 for times 1.4; 1.9; 2.4; 4.1; 7.4; 9.9 and 12.2 hours on stream, respectively, as can be seen in Figure 1.

Briefly surveying the experimental data on the reflectance spectra of $H_4PVMo_{11}O_{40} \cdot x\ H_2O$ under He stream at room temperature (Fig. 1) , we can demonstrate the following characteristic features :

1) With an increase in the time of action of the He flux the water peak intensities at 1430 nm and 1925 nm first decrease and then disappear almost completely after twelve hours of flux action.
2) In the near ultraviolet the $H_4PVMo_{11}O_{40} \cdot x\ H_2O$ compound has a pronounced peak at 400 nm assigned to the LMCT band. In the range 250-540 nm the intensity and the shape of the spectrum do not change during the action of the helium stream. In the range of 600-1300 nm an asymmetrical broad band is observed. Its width significantly exceeds the width of the bands arising from the d-d transitions [9]. The maximum of this band is located in the range of 740-780 nm; a shoulder can be distinguished in the range of 900-1000 nm. We can also see from Fig. 1 that the spectrum intensity in Vis and NIR increases with the time on stream.

It should be stressed, however, that thus far the explanation of the optical spectra of heteropoly compounds has been based only on qualitative and semiempirical considerations. The assignment of intervalence charge transfer bands in the Vis and NIR range was made with the aid of the Jorgensen formula [10-12]. However this assignment is not convincing because the optical electronegativities for

metal ions are not essentially constant values and depend on the nearest ligand surrounding as well as on the type of the solvent in the case of a complex in solution. For that reason, we will advance a vibronic model of the optical spectra of mixed heteropoly acids below, with which we shall attempt to explain the observed spectra particularities and to show which information concerning mixed heteropolyacids can be extracted from the analysis of these spectra.

3. Qualitative Discussion

The quantitative determination of the vanadium (IV) content by EPR shows [13] that in the untreated heteropoly compounds vanadium is present as V(IV), and its amount is about 0.5-2 mol-%. In addition, the EPR spectra evidence proves that the removal of water by a He stream at room temperature for 24 hours does not change the degree of reduction. This is also confirmed by the fact that the intensity of the lowest energy charge transfer band (400 nm) is not diminished, as occurs when reduction takes place. Thus we may conclude that under a He stream the increase of the spectra intensity of HPA in the Vis and NIR range at room temperature is connected with water loss. With water removal the screening of electronic interaction between d^0 and d^1 transition metal ions is taken off, and the overlap of the orbitals of the adjacent d-ions increases, while the mean distance between these ions diminishes. This in turn facilitates the electron transfer. For example, the experimental data of paper [14] show that with a temperature increase in $H_4PVMo_{11}O_{40} \cdot 13\ H_2O$ water loss occurs, and the mean dis-

tance between transition metal ions in the crystal unit cell decreases from 4.43 Å to 3.97 Å if each polyanion is assumed to contain 12 metal ions.

The V^{5+} ions are easily reduced, and therefore the electrons added to V-substituted Keggin polyanions are localized on the vanadiums. In the heteronuclear pair V-Mo the vanadium ion plays the role of a donor insofar as the ionization potentials of molybdenum are higher than those of vanadium [15]. On the other hand, as was stated above, vanadium can substitute addenda in the Keggin unit or be contained in the secondary structure. Different types of V-Mo-dimers may be formed particularly edge-shared and corner-shared dimers in the Keggin polyanion. Much less is known about the V-Mo-dimer when V is located in the secondary structure. In order to avoid the overparameterization of the theory we employ a simplified model dealing with a corner-shared V-Mo bioctahedron for which the transfer processes are most efficient. Thus a first step will consider only an intervalence $V^{4+} – Mo^{6+}$ optical transition involving the electron transfer through a corner. The electron pathways through edges involve $V^{4+} – O – Mo^{6+}$ angles close to the orthogonality value (in range 90-100°) which are unsuited to support the electron transfer and may provide less intensive intervalence optical transitions $V^{4+} – O – Mo^{6+} \rightarrow V^{5+} – O – Mo^{5+}$. Insofar as the concentration of V^{4+} ions is very low [13] at room temperature under helium stream, a model of an isolated $V^{4+} – Mo^{6+}$ -cluster will be accepted below. The reason why the charge transfer band associated with the homonuclear pair $Mo^{5+}–Mo^{6+}$ is not taken into account will be discussed in section 5. It should be also noted

that the calculations of optical spectra of such large molecules as a Keggin unit present very difficult issues and demand very much CPU time. Therefore we model the whole Keggin molecule by subunits. In so far as in the case of consideration the probability of finding two neigbouring V ions within a polyanion is negligibly small, we consider the substitution of only one Mo –ion in our model clusters. As it will be shown this model reproduces the main characteristics of the HPA optical spectra.

In the range of spectra under examination the intensities of the d-d transitions in V^{4+} and Mo^{5+} ions are not negligible. According to structural data in heteropoly compounds of Keggin type as well as in complexes of vanadyl and molybdenyl type the site symmetry of Mo and V ions is close to C_{4v} [16-18]. The component of the crystal field describing the deviation from the C_{4v} symmetry is not appreciable. This component does not lead to new physical effects in optical spectra and can be neglected with good accuracy. Under this assumption the orbitals of the d^1-ion transform according to the irreducible representations b_2 , b_1, e and a_1 of the C_{4v} group, as can be seen in Figure 2. At least three optical d-d transitions between these one-electron states can be observed: I. $b_2 – e$; II. $b_2 – b_1$, III. $b_2 – a_1$. Transition III is most probable in the range of 25000 – 30000 cm^{-1} and usually overlaps with the ligand-metal charge transfer band. However for V^{4+} and Mo^{5+} complexes with a double M=O bond transitions I and II fall inside the spectra range 400 – 900 nm [19] and should be taken into

account along with the intervalence optical transition V^{4+}–O–Mo^{6+}→ V^{5+}–O–Mo^{5+}. Thus the absorption spectrum of the mixed HPA is supposed to consist of a charge transfer band and d-d transitions belonging to V^{4+} and Mo^{5+} ions, and the model suggested below takes this fact into account. It should be stressed that previous papers consider either the charge transfer band or the d-d-transitions [9, 20,21]. A common consideration of these optical bands of different nature has not yet been performed.

The model

Here we consider a dimeric cluster formed by V^{4+} and Mo^{6+} ions. The point symmetry of each cluster ion is assumed to be C_{4v}. The electronic configuration of this cluster is $d^0 – d^1$. In what follows the ions of the cluster will be denoted by the letters a and b. The Hamiltonian of this cluster has the form:

$$\mathcal{H} = H_e + H_{eL} + H_L \qquad (1)$$

where H_e is the electronic Hamiltonian including the interaction of the excess electron with its own and another center as well as the interaction with the crystal field, H_{eL} is the Hamiltonian of electron-vibrational interaction and H_L is the Hamiltonian of free crystal vibrations.

The energy spectrum of each cluster subunit consists of three electronic levels with wave functions φ_{cb2}, $\varphi_{ce\gamma}$, φ_{cb1}, where c = a, b labels the cluster moieties, the symbols b_2, e and b_1 have the same meaning as in Fig.2 , and γ enumer-

ates the basic functions of the representation e. Further, for the sake of simplicity we introduce the following notations:

$$\Phi_1=\varphi_{ae\gamma} \quad , \quad \Phi_2=\varphi_{be\gamma} \quad , \quad \Phi_3=\varphi_{ab1} \quad , \quad \Phi_4=\varphi_{bb1} \qquad (2)$$

In the basis of the functions φ_{cb2} (c=a,b) , Φ_i (i=1,2,3,4) the matrix of the electronic Hamiltonian H_e contains a single two-dimensional non-diagonal block

$$\begin{pmatrix} \varphi_{ab2} & \varphi_{bb2} \\ 0 & p \\ p & w \end{pmatrix}$$

The diagonal matrix elements $< \varphi_{bb2}| H_e| \varphi_{bb2} > = w$, $< \Phi_i | H_e| \Phi_i > = \Delta_i$ (i=1,2,3,4) give the energies of the orbitals φ_{bb2} and Φ_i in the crystal field, these energies are counted from the energy of the orbital φ_{ab2} . The energy gaps w and Δ_i determined in this way depend on the positions of the ions of the host lattice unperturbed by the excess electron. Finally, p is the one-electron transfer parameter. In the simplest case of the only excess electron shared between two atomic cores a and b this parameter is

$$p = \int \varphi_{ab2}(1) \quad \frac{1}{r_{1b}} \quad \varphi_{bb2}(1)\, d\tau_1 \qquad (3)$$

The parameter p reflects the geometry of the cluster and the overlap of the orbitals. The electron transfer between localized states belonging to different irreducible representations of the C_{4v} point group has been neglected. In papers [22,23] the magnitudes of the transfer parameters of such a type were shown to

be small. The transfer of the electron between excited orbitals of the same symmetry is also negligible because the molybdenum orbitals φ_e and φ_{b1} are higher in energy than those of vanadium (see section 5).

As the localized electron strongly perturbs the ligand environment, the vibronic coupling plays a considerable role in mixed-valence systems.

In the PKS model [24,25] operating with two fully symmetric („breathing“) modes of the local environment of each cluster ion (q_a and q_b), the total vibronic operator describing the interaction of these modes with the electronic shells of ions a and b can be expressed as

$$\mathbf{H_{el}} = \upsilon_a(\vec{r})q_a + \upsilon_a(\vec{r})q_b$$

$$= \upsilon_+(\vec{r})q + \upsilon_-(\vec{r})q_- , \qquad (4)$$

where $$\upsilon_{a(b)}(\vec{r}) = \left(\frac{\partial V(\vec{r}, \vec{R})}{\partial q_{a(b)}}\right)_o$$

is the derivative of the potential energy $V(\vec{r}, \vec{R})$ of interaction of the migrating electron with the surrounding ions of the host lattice at the point $q_c = 0$ (c = a, b),

$$\upsilon_\pm(\vec{r}) = (\upsilon_a(\vec{r}) \pm \upsilon_b(\vec{r}))/\sqrt{2}$$

$$q_\pm = (q_a \pm q_b)/\sqrt{2} \qquad (5)$$

In the accepted model the Hamiltonian H_{eL} has only diagonal matrix elements:

$$\langle \varphi_{ab2} \mid \mathbf{H_{el}} \mid \varphi_{ab2} \rangle = \upsilon(q + q_-), \langle \varphi_{bb2} \mid \mathbf{H_{el}} \mid \varphi_{bb2} \rangle = \upsilon(q - q_-)$$

$$\langle \Phi_i \mid \mathbf{H_{el}} \mid \Phi_i \rangle = \upsilon_i(q - (-1)^i q_-) \qquad (6)$$

Here υ_i are the vibronic coupling constants for the excited orbitals Φ_i.The values of the interaction constants with the full symmetric mode q_c (c = a, b) for the orbitals φ_{ab2} and φ_{bb2} are taken to be the same, this approximation is valid as far as the energies of the ground orbitals φ_{ab2} and φ_{bb2} coincide (w =0). The vibronic constants υ and υ_i depend on the positions of the ions surrounding the metal centers a and b in the lattice without the migrating electron.

Finally,

$$\mathbf{H_L} = \sum_{c=a,b} \frac{\hbar\omega}{2} \qquad - \frac{\partial}{\partial} \tag{7}$$

is the Hamiltonian of free lattice vibrations. Then we employed the adiabatic approximation, neglecting the nuclear kinetic energy in the Hamiltonian (7). In this approximation the energies of a dimeric cluster represent the adiabatic potentials. This approach was used in papers [21,26,27] and was shown to give good results when calculating the spectroscopic and thermodynamic characteristics of mixed-valence systems. The molecular adiabatic potentials have the form :

$$\mathbf{u_{\pm}(q_+,q_-) = \pm W(q_-) + \upsilon q + \frac{\hbar\omega}{2} (q^{\hat{}2}+q_-^{\hat{}2}),} \qquad \mathbf{W(q_-) = \sqrt{p^2 + (\upsilon q_-)^2}}$$

$$\mathbf{u_i(q_+,q_-) = \upsilon_i(q - (-1)^i q_-) + \Delta_i + \frac{\hbar\omega}{2} (q^2+q_-^2) \ (i=1,2,3,4)} \tag{8}$$

The wave functions corresponding to the adiabatic potentials $u_{\pm}$ (q_+, q_-) can be expressed as follows :

$$\varphi_{\pm}(q_-) = \{\tfrac{1}{2}(1 \pm \frac{\upsilon q_-}{W(q_-)})\}^{1/2} \varphi_{ab2} \pm \{\tfrac{1}{2}(1 \pm \frac{\upsilon q_-}{W(q_-)})\}^{1/2} \varphi_{bb2} \tag{9}$$

For adiabatic potentials u_i (q_+, q_-) (i = 1, 2, 3, 4) the wavefunctions are Φ_i. We see that the antisymmetric q_- (out – of – phase) mode mixes the tunnel states $(\varphi_{ab2} + \varphi_{bb2})/\sqrt{2}$ and $(\varphi_{ab2} - \varphi_{bb2})/\sqrt{2}$ and leads to the pseudo-Jahn-Teller effect for the whole cluster.

The semiclassical adiabatic approximation is also used for the calculation of the absorption band shapes. The absorption band shape is determined by the relation

$$\mathbf{F(\Omega) = F_{ct}(\Omega) + F_{dd}(\Omega)} \qquad \mathbf{(10)}$$

where

$$\mathbf{F_{ct}(\Omega) = Z^{-1} \iint dq\ dq_- |<\varphi\ (q_-)|d|\varphi_-(q_-)>|^2 \exp[-\frac{u_-(q\ ,q_-)}{kT}]d(u\ (q\ ,q_-) - u_-(q\ ,q_-) - \hbar\Omega)} \qquad \mathbf{(11)}$$

describes the so called charge transfer band (or intervalence transition band), and Z is the partition function. The form-function

$$\mathbf{F_{dd}(\Omega) = Z^{-1} \sum_{i=1}^{4} \iint dq_+ dq_- (|<\Phi_i|d|\varphi_-(q_-)>|^2 \exp[-\frac{u_-(q\ ,q_-)}{kT}]}$$

$$\mathbf{d(u_i(q_+,q_-) - u_-(q\ ,q_-) - \hbar\Omega) + |<\Phi_i|d|\varphi_+(q_-)>|^2 \exp[-\frac{u\ (q_+,q_-)}{kT}]}$$

$$\mathbf{d(u_i(q\ ,q_-) - u\ (q\ ,q_-) - \hbar\Omega)} \qquad \mathbf{(12)}$$

takes into account all transitions from the states $\varphi_-(q_-)$ and $\varphi_+(q_-)$ to the excited localized states. In Eqs. (11) and (12) d is the operator of the cluster effective di-

pole moment. The contribution to the absorption band from the transitions between the excited localized states Φ_i is not taken into consideration insofar as their Boltzman population is negligibly small. For this reason the expression for the partition function Z is as follows :

$$Z = 2\exp\left[\frac{\upsilon^2}{2kT\hbar\omega}\right]\left(\frac{2\pi kT}{\hbar\omega}\right)^{1/2}\int_{-\infty}^{\infty} dq_- \cosh\left(\frac{W(q_-)}{kT}\right)\exp\left(-\frac{\hbar\omega}{2kT}q_-^2\right) \quad (13)$$

Carrying out the integration in Eq. (11) for the form-function of the charge transfer band, we obtain the same formula as in papers [20,28].

$$F_{ct} = \frac{4p^2 d_0^2}{\upsilon Z\hbar\Omega[(\hbar\Omega)^2-4p^2]^{1/2}}\exp\left[\frac{\hbar\omega p^2}{2kT\upsilon^2}\right]\exp\left[-\frac{\hbar\omega}{8kT\upsilon^2}\left(\hbar\Omega - \frac{2\upsilon^2}{\hbar\omega}\right)^2\right]$$
$$\exp\left[\frac{\upsilon^2}{kT\hbar\omega}\right]\left(\frac{2\pi kT}{\hbar\omega}\right)^{1/2} \quad (14)$$

Here $d_0 = eR_o/2$ is the dipole moment of the cluster with the localized electron, and R_o is the distance between the cluster ions. In the case of $\hbar\Omega \gg 2|p|$ the intervalence transition band has one maximum at the point

$$(\hbar\Omega)_{max} = \frac{\upsilon^2}{\hbar\omega} + \left[\left(\frac{\upsilon^2}{\hbar\omega}\right)^2 - \frac{8kT\upsilon^2}{\hbar\omega}\right]^{1/2} \quad (15)$$

For the form-function $F_{dd}(\Omega)$ describing the contribution of the d-d-transitions after integration over q_+ we obtain

$$F_{dd}(\Omega) = 2\overline{|\langle\varphi_{ab2}|d|\varphi_{ae}\rangle|^2}\, I(\Omega, \upsilon_1) + 2\overline{|\langle\varphi_{bb2}|d|\varphi_{be}\rangle|^2}\, I(\Omega, \upsilon_2) +$$
$$|\langle\varphi_{ab2}|d|\varphi_{ab1}\rangle|^2 I(\Omega, \upsilon_3) + |\langle\varphi_{bb2}|d|\varphi_{bb1}\rangle|^2 I(\Omega, \upsilon_4) \quad (16)$$

Insofar as nonpolarized light is applied to the system, the „oscillator strengths“ $|\langle\varphi_{cb2}|\,\mathbf{d}\,|\varphi_{ce\gamma}\rangle|^2$ are replaced by the value averaged over directions of light polarization. The integrals $I(\Omega, \Delta_i, v_i)$ have the form :

$$I(\Omega, \Delta_i, \upsilon_i) = \exp\left[\frac{\upsilon(\Delta_i - \hbar\Omega)}{(\upsilon_i - \upsilon)kT}\right] \frac{1}{2|\upsilon_i - \upsilon|Z}$$

$$\int_{-\infty}^{\infty} dq_-\left(1 + \frac{\upsilon q_-}{W(q_-)}\right) \exp\left[-\frac{\hbar\omega}{2kT} q_-^2\right]$$

$$\left\{\exp\left[-\frac{\upsilon\upsilon_i q_-}{(\upsilon_i - \upsilon)kT}\right] \exp\left[\frac{\upsilon_i}{(\upsilon_i - \upsilon)kT} W(q_-)\right]\right.$$

$$\exp\left[-\frac{\hbar\omega}{2kT(\upsilon_i - \upsilon)^2} (\hbar\Omega - W(q_-) - \Delta_i + \upsilon_i q_-)^2\right]$$

$$+\exp\left[\frac{\upsilon\upsilon_i q_-}{(\upsilon_i - \upsilon)kT}\right] \exp\left[-\frac{\upsilon_i}{(\upsilon_i - \upsilon)kT} W(q_-)\right]$$

$$\left.\exp\left[-\frac{\hbar\omega}{2kT(\upsilon_i - \upsilon)^2} (\hbar\Omega + W(q_-) - \Delta_i - \upsilon_i q_-)^2\right]\right\} \qquad (17)$$

From Eqs. (14) and (17) we see that in the case of noticeable electron transfer the spectrum represents a superposition of a charge transfer band and 8 optical transitions between the tunnel states $\varphi_\pm$ and the excited localized states $\varphi_{ce\gamma}$ and φ_{cb1} (c = a, b). From Eq. (17) it is seen that appreciable transfer parameters affect significantly the shapes of the d-d-bands. When the transfer parameter p is negligibly small in comparison with the vibronic parameter υ ($\upsilon^2/\hbar\omega \gg p$) we obtain from Eq. (16) 4 „pure“ d-d transitions. Each d-d transition is described by a Gaussian curve :

$$I(\Omega, \Delta_i, \upsilon_i) = \frac{1}{4|\upsilon_i - \upsilon|} \sqrt{\frac{\hbar\omega}{\pi kT}} \exp\left[-\frac{\hbar\omega}{4kT(\upsilon_i - \upsilon)^2}\right.$$

$$*(\ \hbar\Omega_m - \hbar\Omega)^2] \qquad (18)$$

$$\hbar\Omega_m = \ _i \ - \ \frac{2\,\upsilon\,(\upsilon_i - \upsilon)}{\hbar\omega} \qquad (19)$$

The energy $\hbar\Omega_m$ of the maximum of the band should be attributed to the observed gap between the levels involved in the optical transition. The gap Δ_i is redetermined as a result of the d-electron shifting the ligands to new equilibrium positions.

5. The values for the parameters

The band shape of the optical absorption of the dimeric cluster under examination depends on the mutual arrangement of the adiabatic potential sheets $u_{\pm}$ (q_+, q_-), u_i (q_+, q_-) and is governed by 15 parameters υ, p, Δ_i, υ_i, ω, $|\langle\varphi_{c\Gamma\gamma}|\,d\,|\varphi_{c\Gamma'\gamma'}\rangle|^2$. In order to calculate the form of the spectrum in the Vis and NIR range of light we will first try to evaluate and discuss the values of the above-mentioned parameters.

We start with the determination of the vibronic parameters υ, υ_i and the gaps Δ_i. The difference between the sixth ionization potential of Mo (67 eV) and the fifth ionization potential of V (65.2 eV) for free atoms is 1.8 eV [15]. This value can be significantly reduced in a coordination compound. Therefore the band at 900-1000 nm has been assigned to the V^{4+} -Mo^{6+} heteronuclear pair. This assignment is consistent with the trends in the reduction potentials and the gaps between HOMO and LUMO in the V-substituted Keggin ions [29]. The charge transfer band for the homonuclear Mo^{5+} – Mo^{6+} pair is expected to be at

essentially lower energy. This band probably has a much lower intensity and cannot be resolved.

The maximum of a charge transfer band is connected with the vibronic parameter υ by the relation (15). In the case of ω = 1000 cm^{-1} [3] at room temperature for the charge transfer band corresponding to the V-Mo –dimer we obtain the value v = 2318 cm^{-1} for the vibronic coupling constant. For single complexes of vanadyl and molybdenyl type the energy of the d-d-transition b_2-e varies in the ranges 11000-14500 cm^{-1} and 12800-15500 cm^{-1}, respectively [19]. For the transition b_2 –b_1 for both V^{4+} and Mo^{5+} the energies are higher and of the order of 16000-23000 cm^{-1}. In fact, the main features of the spectra of vanadyl complexes are strikingly similar [19] ;a band at about 13000 cm^{-1} followed by a second band at about 16000-17000 cm^{-1}. For instance, for the complex $[VO(H_2O)_5]^{2+}$ contained under certain conditions in vanadium substituted HPA [3,4,13] the energies of the transitions b_2-e and b_2 –b_1 are 13000 cm^{-1} and 16000 cm^{-1} [30], respectively. Meanwhile, the bands arising from the transition b_2-e are more intensive in so far as the transition b_2-e is dipole allowed while the transition b_2 –b_1 is dipole forbidden. Thus for the complex $[VO(H_2O)_5]^{2+}$ the oscillator strengths correspondingly have the values $1.1*10^{-4}$ and $0.45*10^{-4}$ for the transitions b_2-e and b_2 –b_1 [30]. Proceeding from these data we assign the maximum in the range 740-780 nm to the b_2-e transitions in V^{4+} and Mo^{5+}-ions. There is a further point to be made in support of this assumption. Generally based on the data of electronegativities a conclusion is drawn that the V-Mo

charge transfer band is situated in the range of 13000-14000 cm^{-1}. Nevertheless this phenomenological assignment cannot be considered as a rule. It was shown above that the position of the charge transfer band and its intensity actually depend on two microscopic parameters υ and p reflecting the symmetry of the nearest environment of the d ions, the symmetry and overlap of the orbitals of interacting ions (see Eqs. (14),(15)). Even if a charge transfer band is assumed to be in the range of 13000-14000 cm^{-1}, its intensity should grow due to the increase of the transfer parameter with removal of water. In this case, owing to the close position of this broad band to the LMCT band, the latter should also intensively increase in a wide spectral interval. However this effect is not confirmed by the experimental data. The LMCT band increases only insignificantly on its edge as seen in Fig.1. In such a way, qualitative considerations and experimental data on vanadyl and molybdenyl complexes cause us to conclude that in the Vis range the d-d-transitions contribute significantly to the full absorption band. Unfortunately at room temperature the spectrum in the Vis and NIR range cannot be deconvoluted into the d-d-bands and the charge transfer band. This makes impossible the semiempirical determination of the vibronic constants υ_i from the half-width of the d-d-bands (see, for example, Eq. (18)). That is why the crystal field theory is employed further for the calculation of the vibronic constants υ_i and the gaps Δ_i .

As was noted above for each metal ion of the cluster, the symmetry of the nearest surrounding is assumed to be close to the symmetry C_{4v}. The distortion

axis (z) lies along the shortest M=O double bond (R_1 (M=O) ≈ 1.68 Å) as can be seen in Figure 3. Four oxygens lie in the xy plane (R (M-O) ≈1.93 Å), and the sixth oxygen is much farther away (R_2 (M-O) ≈ 2.32 Å) below the equatorial plane [16-18]. The radia R, R_1, R_2 relate to the ions V^{5+} and Mo^{6+} with the unfilled d-shell, for the first approximation these radia are taken to be the same. For the complex shown in Fig.3, in the point charge model of the crystal field the energies of the orbitals are defined as follows:

$$\varepsilon_{a1}^{c} = 6Dq^{c} + \frac{2}{7} f_1^{c}(R_1,R_2,R) + \frac{2}{7} f_2^{c}(R_1,R_2,R)$$

$$\varepsilon_{e}^{c} = -4Dq^{c} - \frac{4}{21} f_1^{c}(R_1,R_2,R) + \frac{1}{7} f_2^{c}(R_1,R_2,R)$$

$$\varepsilon_{b2}^{c} = -4Dq^{c} + \frac{1}{21} f_1^{c}(R_1,R_2,R) - \frac{2}{7} f_2^{c}(R_1,R_2,R) \qquad (20)$$

where

$$Dq^{c} = \frac{ze^2\langle r^4\rangle_c}{6R^5} \quad ;$$

$$f_1^{c}(R_1,R_2,R) = ze^2\langle r^4\rangle_c \left(\frac{1}{R_1^5} + \frac{1}{R_2^5} - \frac{2}{R^5} \right)$$

$$f_2^{c}(R_1,R_2,R) = ze^2\langle r^2\rangle_c \left(\frac{1}{R_1^3} + \frac{1}{R_2^3} - \frac{2}{R^3} \right) \qquad (21)$$

$\langle r^4\rangle_c$ and $\langle r^2\rangle_c$ are the radial integrals for the ion c with the localized electron, while R, R_1 ,R_2 , as was mentioned above, refer to the ligand positions in the absence of the d-electron. For each cluster subunit (a or b) the operator υ_c (r) (see

Eq. (4)) of interaction with the full symmetric vibrations of the nearest surrounding can be expressed as a derivative of the crystal field potential at $q_c = 0$.

For the matrix elements of this operator we obtain :

$$\upsilon_c^{b2} = \sqrt{\frac{\hbar\omega}{6f_c}}\left(20\ \frac{Dq^c}{R} + \frac{1}{21} f_3^c(R_1,R_2,R) - \frac{2}{7} f_4^c(R_1,R_2,R)\right)$$

$$\upsilon_c^{b1} = \sqrt{\frac{\hbar\omega}{6f_c}}\left(-30\ \frac{Dq^c}{R} + \frac{1}{21} f_3^c(R_1,R_2,R) - \frac{2}{7} f_4^c(R_1,R_2,R)\right)$$

$$\upsilon_c^{a1} = \sqrt{\frac{\hbar\omega}{6f_c}}\left(-30\ \frac{Dq^c}{R} + \frac{2}{7} f_3^c(R_1,R_2,R) + \frac{2}{7} f_4^c(R_1,R_2,R)\right)$$

$$\upsilon_c^{e} = \sqrt{\frac{\hbar\omega}{6f_c}}\left(20\ \frac{Dq^c}{R} - \frac{4}{21} f_3^c(R_1,R_2,R) + \frac{1}{7} f_4^c(R_1,R_2,R)\right) \quad (22)$$

where f_c is the mean force constant of the full symmetric vibration for the ion c,

$$f_3^c(R_1,R_2,R) = -5ze^2\langle r^4\rangle_c \left(\frac{1}{R_1^6} + \frac{1}{R_2^6} - \frac{2}{R^6}\right)$$

$$f_4^c(R_1,R_2,R) = -3ze^2\langle r^2\rangle_c \left(\frac{1}{R_1^4} + \frac{1}{R_2^4} - \frac{2}{R^4}\right) \quad (23)$$

The vibronic coupling constants (22) and the energies of the orbitals (20) are connected with the parameters υ ,υ_i and Δ_i (i = 1-4) introduced in section 4 by simple relations :

$\upsilon = \upsilon_c^{b2}/\sqrt{2}$; (c = a,b);

$\upsilon_1 = \upsilon_a^{e}/\sqrt{2}$; $\upsilon_2 = \upsilon_b^{e}/\sqrt{2}$; $\upsilon_3 = \upsilon_a^{b1}/\sqrt{2}$; $\upsilon_4 = \upsilon_b^{b1}/\sqrt{2}$;

$\Delta_1 = \varepsilon_{ae} - \varepsilon_{ab2}$, $\Delta_2 = \varepsilon_{be} - \varepsilon_{bb2}$, $\Delta_3 = \varepsilon_{ab1} - \varepsilon_{ab2}$, $\Delta_4 = \varepsilon_{bb1} - \varepsilon_{bb2}$ **(24)**

The point charge model of the crystal field applied for the derivation of the formulae (20) and (22) correctly takes into account all symmetry aspects, but does not describe the covalency effects. In the framework of this model the covalency effects can be accounted for quantitatively by the determination of the radial integrals $\langle r^2 \rangle_c$ and $\langle r^4 \rangle_c$ in a semiempirical manner [19]. Here we apply the following procedure for the estimation of these integrals. Substituting (20) and (22) in (24) with the aid of Eq. (19) and experimental data on the maxima of the d-d- bands (transitions $b_2 - e$, $b_2 - b_1$) in complexes $[VO(H_2O)_5]^{2+}$ and $[MoOCl_5]^{2-}$ [19,30] we obtain the semiempirical values for the radial integrals $\langle r^2 \rangle_c$ and $\langle r^4 \rangle_c$ and then calculate with these values the parameters Δ_i and υ_i listed in Table 1. The radial integrals thus obtained fit the value for the parameter υ calculated above. As the complexes MoO_6 in the Keggin unit the complex $[MoOCl_5]^{2-}$ is of molybdenyl type with a double M=O bond, its $b_2 - e$- band falls in the same range [30] with the observed maximum at 740-780 nm in the HPA. Therefore the estimation of the radial integrals for Mo^{5+} carried out seems to be reasonable. As to the $[VO(H_2O)_5]^{2+}$ complex the use of its band positions when determining the radial integrals is justified by the fact that in this complex the V-ion is surrounded by 6 oxygens. Besides this the complex may be a component of the HPA [3,4,13]. The values of the matrix elements $\left| \langle \varphi_{c\Gamma} \left| d \right| \varphi_{c\Gamma'} \rangle \right|^2$ of the effective dipole moment (Table 2) were obtained from the experimental values for the oscillator strengths in $[MoOCl_5]^{2-}$ and

$[VO(H_2O)_5]^{2+}$ complexes [30]. Unfortunately to our knowledge there is no experimental data in the literature on oscillator strengths and band positions in complexes containing MO_6 units with a double Mo=O bond.

6. Numerical Simulation of the Absorption Spectra of HPA

Intensity calculations

In Figure 4 the calculated and experimental absorption spectra of the HPA are shown for different times on stream. The spectra simulation was carried out in the Vis and NIR range. The calculated spectra were obtained by summation of the contributions from the charge transfer band and d-d-transitions (see Eqs. (10)- (17)). The values for the parameters Δ_i, υ_i, υ and $\left|<\varphi_{c\Gamma}\right| d \left|\varphi_{c\Gamma'}>\right|^2$ were taken from Tables 1 and 2. When calculating the spectra for different times on helium stream the transfer parameter was considered as a fitting parameter. The distance R_o between the cluster ions was taken to be equal to 3.71 Å as for corner-sharing octahedra [1] in the Keggin unit. From Fig. 4 it is seen that the longer the time on helium stream and the larger the transfer parameter, the better the fit of the experimental curve. This result can be explained as follows. The secondary HPA crystal structure consists of layers of crystal water between the Keggin ions. The water molecules binding the Keggin units together and forming water bridges screen and weaken the interaction of the addenda ions within the Keggin unit. Cases are known in which terminal oxygens are replaced by water ligands [31]. That is why the electron transfer is partially

suppressed at the beginning of the experiment. The loss of crystal water is accompanied by different structural transformations [14,32,33] that result in the increase of the overlap of the orbitals of the adjacent ions as well as in the decrease of the mean distance between addenda ions [14] in the unit cell of the crystal. As a consequence the electron transfer parameter increases with time on stream. Unfortunately we do not have information on the change in the mean distance between the metal ions in the examined compound under He stream. Therefore we fix the distance R_o between cluster ions and fit only the transfer parameter p. The obtained p values satisfy the relationship $\upsilon^2/\hbar\omega \gg p$, $\hbar\Omega \gg 2$

p. In this case (see Eqs. (14),(18)) under change in the distance between cluster ions from R_o to R_o' the results of calculation for the shapes [Fig.4] and intensities of all spectra will remain the same, if the transfer parameter determined afresh $p' = p\, R_o/R_o'$ also satisfies the inequality $\upsilon^2/\hbar\omega \gg p'$.

As is seen from Fig. 4 in the range 630 nm < λ < 1200 nm for spectra 3-7 recorded from 2.4 to 12.2 hours on stream the calculated band curves are in good agreement with the observed ones.

Here some comments should be made concerning other spectra. Vis and NIR intensities could only be observed after a time on stream of 2.4 hours and the NIR intensity changes very little initially. For that reason, it is assumed that a certain induction period for observable d-d and charge transfer transitions is necessary.

From Fig. 4 we can also see that for spectra recorded in the interval from 2.4 to 12.2 hours on stream in the range of $\lambda > 1200$ nm a discrepancy is observed between the theoretical and experimental curves. The possible explanation for this discrepancy is the existence in this range of a weak intensity charge transfer band arising from the intervalence optical transition $Mo^{5+} - O - Mo^{6+} \rightarrow Mo^{6+} - O - Mo^{5+}$. To obtain the shape of the total spectra of 250 nm $< \lambda <$ 610 nm, one should take into consideration the lowest energy charge transfer band and the band associated with the d-d transition $b_2 - a_1$, because an overlap of these bands and the bands arising from the $b_2 - b_1$ transitions takes place in the

range of 350 – 610 nm. The increase of the LMCT band on its edge is probably connected with the change of the band gap energy with water removal. Figure 5 shows the individual contributions of the charge transfer band and the d-d-transitions to the spectrum 5 obtained after 7.4 hours on stream. We see that the bands corresponding to the d-d-transitions are symmetric and have the Gaussian forms, as far as for all these curves $\upsilon^2/\hbar\omega \gg p$. It is also evident that the contributions of the d-d-transitions to the full spectra are comparable to those of the intervalence transitions.

The most important characteristic of an absorption band is its zeroth moment, which measures the integrated intensity (area). We investigate here the variation of the intensity of spectra recorded at different times on helium flux. For each spectrum we calculate the intensity in the range of 612 nm $< \lambda <$ 1340 nm using

the theoretical formulae (10) –(17). In order to compare the theoretical results with the experimental ones we introduce a parameter n_i, characterizing the relative intensity increase of spectrum i :

$$n_i = I_i / I_0 \qquad (25)$$

here I_0 is the intensity of the spectrum 7 measured after 12.2 hours on stream. The calculated and experimental values of the parameter n_i are shown in Figure 6. One can see a good coincidence of the theoretical and experimental points.
The theoretical calculations also make it possible to separate the contributions of the d-d transitions and the charge transfer band from the total spectrum intensity.

In Table 3 the relative contributions from the d-d transitions and the charge transfer band to the total spectra intensities are listed for spectra recorded in the interval of time on stream from 1.4 to 12.2 hours. We see that the relative contribution of the d-d transitions decreases appreciably with time on stream, while the intensity of the charge transfer band grows with the increase in the transfer parameter.

Concluding remarks

A model of a mixed-valence V^{4+}-Mo^{6+} dimeric cluster has been proposed to describe the evolution of the absorption bands of mixed HPA compounds under action of the flux of an inert gas and temperature. The following relevant electronic processes and interactions were taken into account :

a) electron transfer processes;

b) vibronic interactions of the transition metal ions with the full symmetric displacements of the nearest surrounding;

c) the interaction of the transition metal ions with the crystal field.

The inputs for the task were : the unit cell structure, the change of the EPR spectra under temperature and inert gas flux, the UV/Vis/NIR spectra for variable-time of the He flux from 1.4 to 12.2 hours at room temperature. The site symmetry of the cluster ions was supposed to be C_{4v}, the energy spectrum of each ion was assumed to consist of three levels with the symmetry b_2 ,e, b_1.

The main results of the consideration can be summed up as follows:

In the adiabatic approximation the full pattern of the energy spectrum for a single cluster is obtained as a superposition of adiabatic potential sheets. This approximation is also employed for the quantum-mechanical calculation of the absorption band-shape in the Vis and NIR part of the spectra. For high temperatures and strong electron-vibrational interaction, which were considered in the problem examined, this approximation is valid. The absorption spectrum is shown to be a superposition of the charge-transfer band and optical d-d transitions. For appreciable transfer parameter values the bands corresponding to the d-d transitions are asymmetrical and non Gaussian. In such a way, the coupling between two cluster centers by electron transfer modifies the band-shapes of the

d-d transitions. When the parameter p is small the d-d –bands have the Gaussian form.

The optical band-shapes of the HPA are investigated in detail for different times of action of the inert gas flux. For numerical simulation of the spectra the estimation of the vibronic coupling constants was carried out with the aid of the crystal field theory. Meanwhile, realizing the deficiencies in this theory in order to improve the description the radial integrals necessary for calculating the vibronic parameters were determined in a semiempirical way. There is a further point to be made concerning the vibronic interactions. In [34] a vibrational mode Q_{ab} which appreciably affects the internuclear a-b-bond length in the cluster and changes the transfer parameter was introduced. The introduction of this mode into the theory results in the appearance of a new vibrational parameter, the microscopic calculation of which is difficult and entails a series of new approximations. Thus for the first step for the description of the charge transfer band the simplified PKS-model [24,25] that provides a clear insight in the phonon assisted optical bands and deals only with two parameters υ and p was accepted.

It was shown that the time evolution of the spectra is connected with the increase of the transfer parameter, i.e. with the increase of the interaction of V and Mo ions in the cluster when water is removed. Quite a good agreement of the experimental observations and theoretical calculations shows that the model reflects the main features of the reality. It was also demonstrated that the UV/Vis spectroscopy presents a real possibility for modelling the processes

which take place in the catalyst under different experimental conditions. In contrast, the model of chemical reactions based on the calculations of the molecular orbitals of the catalyst and reactant suggested in [35,36] represents only an assumption that cannot be directly confirmed by experiment.

At the same time in order to discuss the real systems in more detail a generalization is necessary on several points. In the adopted model the covalency effects in the vibronic constants are accounted for by introducing semiempirical values of radial integrals, the oscillator strengths of the d-d-transitions were taken from experimental data on complexes $[MoOCl_5]^{2-}$ and $[VO(H_2O)_5]^{2+}$ [30]. For future calculations of the vibronic coupling constants and oscillator strengths for a MO_6 complex we intend to apply a model that successively takes into account the covalency effects.

The contribution of trimeric clusters of the type of $V^{4+} - Mo^{6+} - Mo^{6+}$, $V^{4+} - V^{4+} - Mo^{6+}$ to the optical spectra should also be taken into account.

As to the transfer parameter its microscopic calculation is not a trivial task, especially for systems that lose water with the change of experimental conditions. Unfortunately, to our knowledge at present there are no methods within the framework of which ab-initio calculations of the energy spectrum, vibronic coupling constants, oscillator strengths and transfer parameters can be performed simultaneously. Meanwhile, in spite of several restricting assumptions made in the consideration carried out above the suggested model accounts for

the main physical factors responsible for the shape transformation of the optical spectra of heteropoly acids under helium stream at room temperature.

References

1. M.T. Pope, Heteropoly and Isopoly Oxometalates,Springer-Verlag, Berlin, 1983.
2. T.Okuhara,N.Mizuno,M.Misono,Adv.Catal.41,113 (1996)
3. D. Casarini, G. Centi, P. Jiru, V. Lena, and Z. Tvaruzkova, J. Catal. ***143***, 325 (1993).
4. T.Bergier,K.Brückman and J.Haber ,Recl.Trav.Chim.Pays-Bas, 113, 475 (1994)
5. S.Berndt, D. Herein, F.Zemlin, E. Beckmann, G. Weinberg, J.Schütze, G.Mestl and R.Schlögl, Ber.Bunsenges.Phys.Chem., 102,763 (1998).
6. J. Melsheimer, Sabri S. Mahmoud, G. Mestl, and R. Schlögl, Catalysis Letters **60**, 103 (1999).
7. M. Thiede and J. Melsheimer, to be published.
8. G.A. Tsigdinos, Ind. Eng. Chem., Proc. Res. Develop. 13 (4), 267 (1974).
9. Yu. E. Perlin, and B.S. Tsukerblat, Optical Bands and Polarization Dichroism of Jahn-Teller centers in Dynamical Jahn-Teller Effect in Localized Systems (Elsevier Publ. B.B. 1984).
10. C.K. Jorgensen, Mol. Phys. ***2***, 309 (1959).
11. C.K. Jorgensen, Struct. Bonding (Berlin) ***1***, 3 (1966) .
12. H. So and M.T.Pope ,Inorg.Chem. 11,1441 (1972)
13. J. K. Lee, V. Russo, J. Melsheimer, K. Köhler, and R. Schlögl, Phys.Chem.Chem.Phys. 2, 2977 (2000).

14. M. Fournier, C. Feumi-Jantou, Cherifa Rabia, Gilbert Herve, and S. Launay, J. Mater. Chem. ***2***(9), 971 (1992).

15. Holleman-Wiberg, Lehrbuch der Anorganischen Chemie, Berlin, 101. edition, 1995.

16. H.R. Allcock, E.C. Bissel, and E.T. Shawl, Inorg. Chem. ***12***, 2963 (1973).

17. D.D. Dexter, and J.V. Silverton, J. Amer. Chem. Soc. ***90***, 3589 (1968).

18. G.M. Varga, E. Papaconstantinou, and M.T. Pope, Inorg. Chem. ***9*** (3), 662 (1970).

19. A.B.P. Lever, Inorganic electronic spectroscopy, Elsevier, second edition (1984).

20. K.V. Wong, P.N. Schatz, and S.P. Piepho, J. Am. Chem. Soc. ***101***, 2793 (1979).

21. B.S. Tsukerblat, S.I. Klokishner, and B.L. Kushkuley, Chem. Phys. ***166***, 97 (1992).

22. M.I. Belinsky and B.S. Tsukerblat, Fiz. Tverdogo Tela ***26,*** 758 (1984); Khim. Fiz. ***4,*** 606 (1985).

23. M.I. Belinsky, B.S. Tsukerblat, I.G. Botsan, and I.C. Belinskaya, Teor. Exper. Khim. ***2,*** 148 (1987).

24. S.B. Piepho, E.R. Krausz and P.N. Schatz, J. Am. Chem. Soc. ***100***, 2996 (1978).

25. P.N. Schatz, S.B. Piepho, and E.R. Kraucz, Chem. Phys. Lett. ***55,*** 539 (1978).

26. S.I. Klokishner, B.S. Tsukerblat, and B.L. Kushkuley,New J. Chem. ***17***, 43 (1993).

27. S.I. Klokishner, B.S. Tsukerblat, and B.L. Kushkuley, Phys. Lett. A ***179***, 429 (1993).

28. S.I. Klokishner and B.S. Tsukerblat, Spectroscopy Letters ***23***, 637 (1990).

29. R.S.Weber, J. Phys.Chem. 98, 2999 (1994).

30. H. Gray, C.R. Hare, Inorg. Chem. ***1***, 363 (1962).

31. F. Zonnenvijlle, C.M. Tourne, G.F. Tourne, Inorg.Chem. 21,2742 (1982).

32. B.Herzog, W. Bensch, T.Ilkenhans, R. Schlögl and N.Deusch, Cat. Lett., 20, 203 (1993).

33. T. Ilkenhans, B. Herzzog, T. Brown and R.Schlögl, J.Catal. 153,275 (1995).

34. S.B.Piepho, J.Am.Chem.Soc. 110, 6319 (1988)

35. K.Bruckman, J.Haber, E.M.Serwicka, Faraday Discuss.Chem.Soc.87, 173(1989).

36. E.M.Serwicka, E.Broclawik, K.Bruckman and J.Haber, Catalysis Letters 2,351 (1989).

Figure Captions

Fig.1. UV/VIS apparent absorption spectra of the HPA for different times (hrs) on helium stream at 300 K.

1. 1.4 hrs; 2. 1.9 hrs; 3. 2.4 hrs; 4. 4.1 hrs; 5. 7.4 hrs; 6. 9.9 hrs;

7. 12.2 hrs.

Fig.2. Splitting of energy levels of the d^1-ion in the crystal field:

a) cubic field, b) C_{4v} symmetry field.

Fig.3. Approximate environment (idealized to C_{4v} symmetry) of a metal ion in a Keggin polyanion[16-18].

Fig.4. The band shapes of the apparent absorption spectra of the HPA for different times on helium stream at 300 K. The numbering of the spectra corresponds with that in Fig.1 (thin line: theoretical calculation, thick line: experimental results).

Fig.5. Contributions from the d-d-transitions and the charge transfer band to the spectrum 5 recorded after 7.4 hrs on stream at 300 K.

Fig. 6. The dependence of the relative Vis and NIR intensity of the spectra of

the HPA on time on helium stream: ▼ experiment, ■ theory. The theoretical points for spectra 1-7 were calculated with following transfer parameter p values:

1. 111 cm^{-1}; 2. 133 cm^{-1}; 3. 155 cm^{-1}; 4. 173 cm^{-1}; 5. 180 cm^{-1},

6. 187 cm^{-1}; 7. 192 cm^{-1}.

Table Captions

Table 1. Values of the characteristic parameters for the V-Mo cluster.

Table 2. The matrix elements of the effective dipole moment $|\langle\varphi_{c\Gamma}|\mathbf{d}|\varphi_{c\Gamma'}\rangle|^2$ in 10^{-61} SI units.

Table 3. Relative contributions to the intensities of spectra 1-7 from the d-d-transitions and the charge transfer band.

V^{4+}							Mo^{5+}						
$\langle r^2 \rangle$ (Å²)	$\langle r^4 \rangle$ (Å^4)	Δ_1, (cm^{-1})	Δ_3, (cm^{-1})	υ_1 (cm^{-1})	υ_3 (cm^{-1})	f (N/m)	$\langle r^2 \rangle$ (Å²)	$\langle r^4 \rangle$ (Å^4)	Δ_2, (cm^{-1})	Δ_4, (cm^{-1})	υ_2 (cm^{-1})	υ_4 (cm^{-1})	f (N/m)
3.26	0.41	3783	5856	294	126	8	4.94	0.76	5612	10953	495	-176	22

Table 1

Ion	Transition $\Gamma \longrightarrow \Gamma'$	$\left\vert \langle \varphi_{c\Gamma} \vert d \vert \varphi_{c\Gamma'} \rangle \right\vert^2$
V^{4+}	$b_2 \longrightarrow e$ $b_2 \longrightarrow b_1$	2.2 1.4
Mo^{5+}	$b_2 \longrightarrow e$ $b_2 \longrightarrow b_1$	2.2 1.9

Table 2

spectrum	time on stream	relative contribution from the d-d-transition	relative contribution from the charge transfer band
1	1.4	56.7	43.3
2	1.9	52.1	47.9
3	2.4	40.6	59.4
4	4.1	39.4	60.6
5	7.4	37.6	62.4
6	9.9	35.7	64.3
7	12.2	34.7	66.3

Table 3

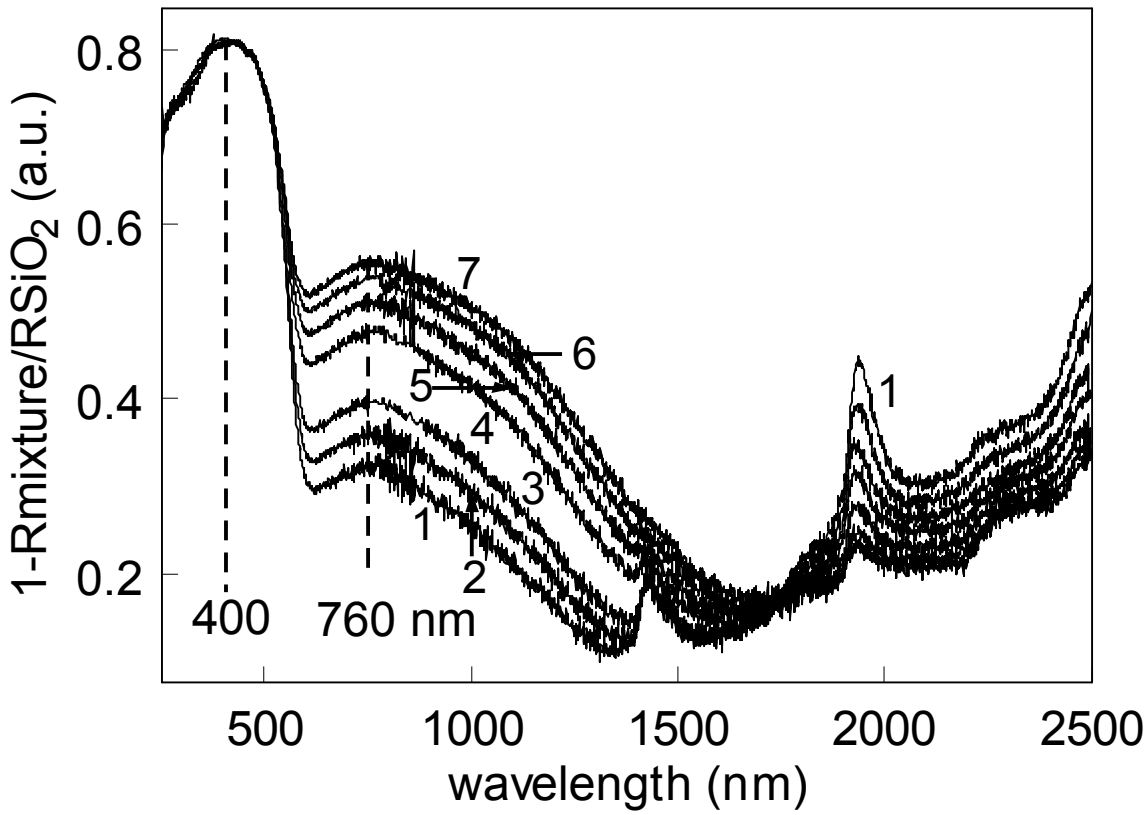
0.8
0.6
0.4
0.2
1-Rmixture/RSiO2 (a.u.)
7
6
5
4
3
1
2
1
400
760 nm
500
1000
1500
2000
2500
wavelength (nm)

Figure 1

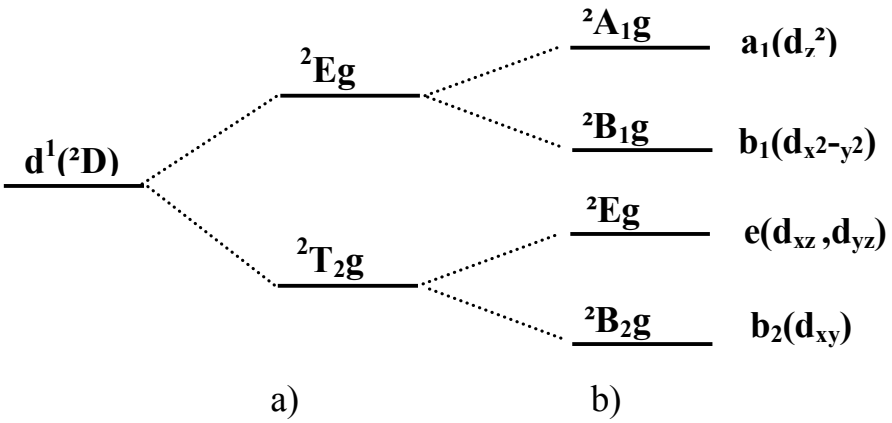
d¹(²D)
²Eg
²T₂g
²A₁g
a₁(d_z²)
²B₁g
b₁(d_x²-y²)
²Eg
e(d_xz ,d_yz)
²B₂g
b₂(d_xy)
a)
b)

Figure 2

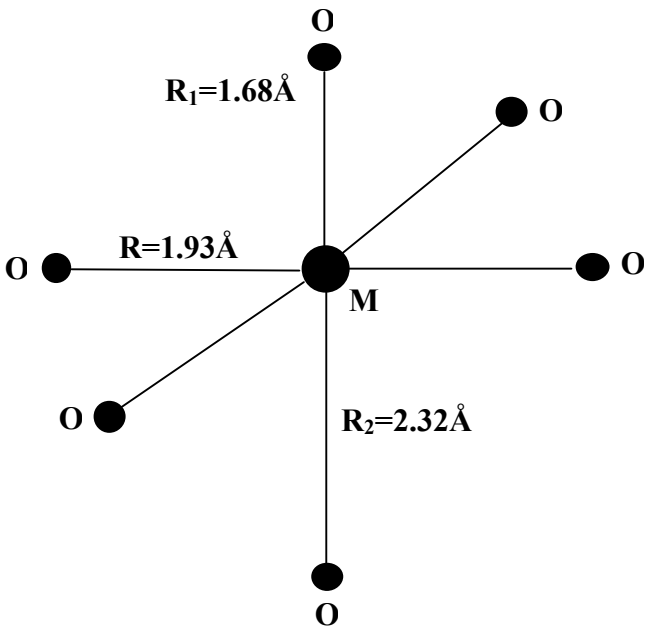

Figure 3

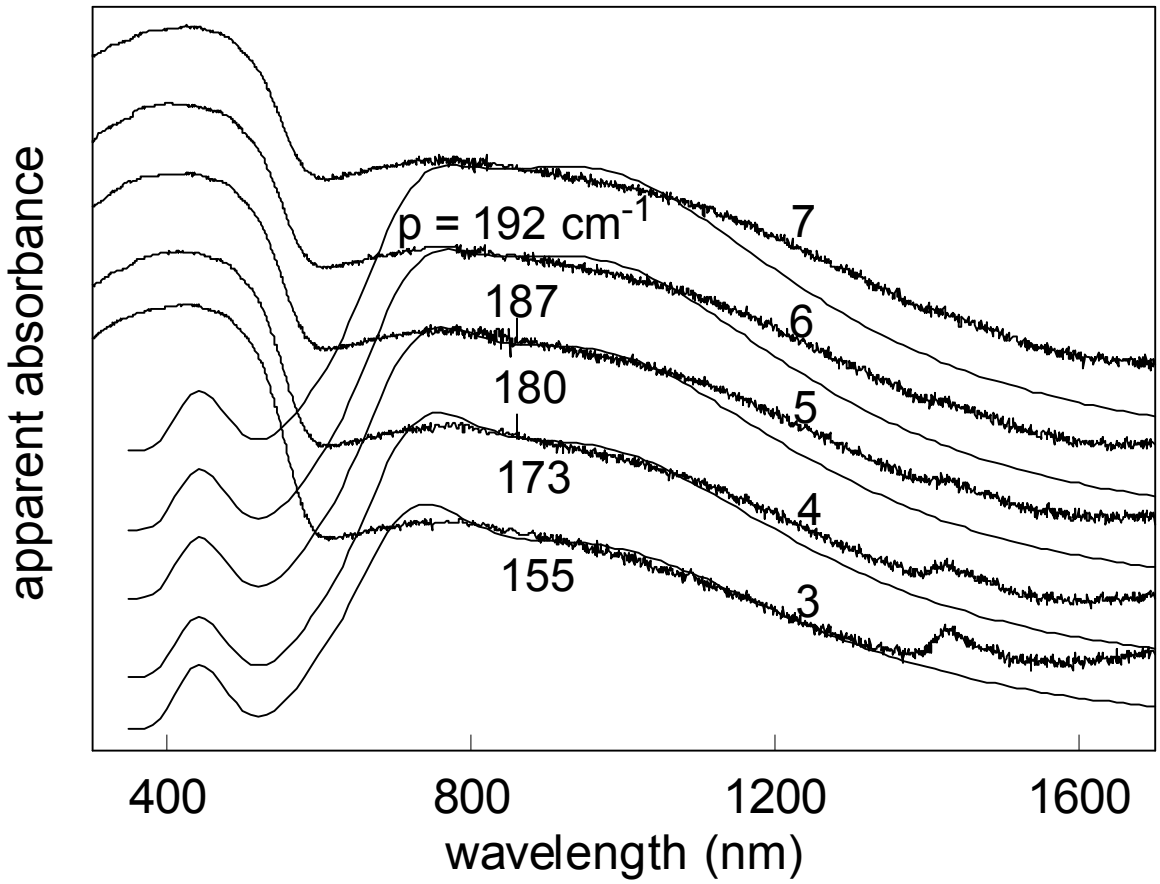
apparent absorbance
p = 192 cm-1
187
180
173
155
7
6
5
4
3
400
800
1200
1600
wavelength (nm)

Figure 4

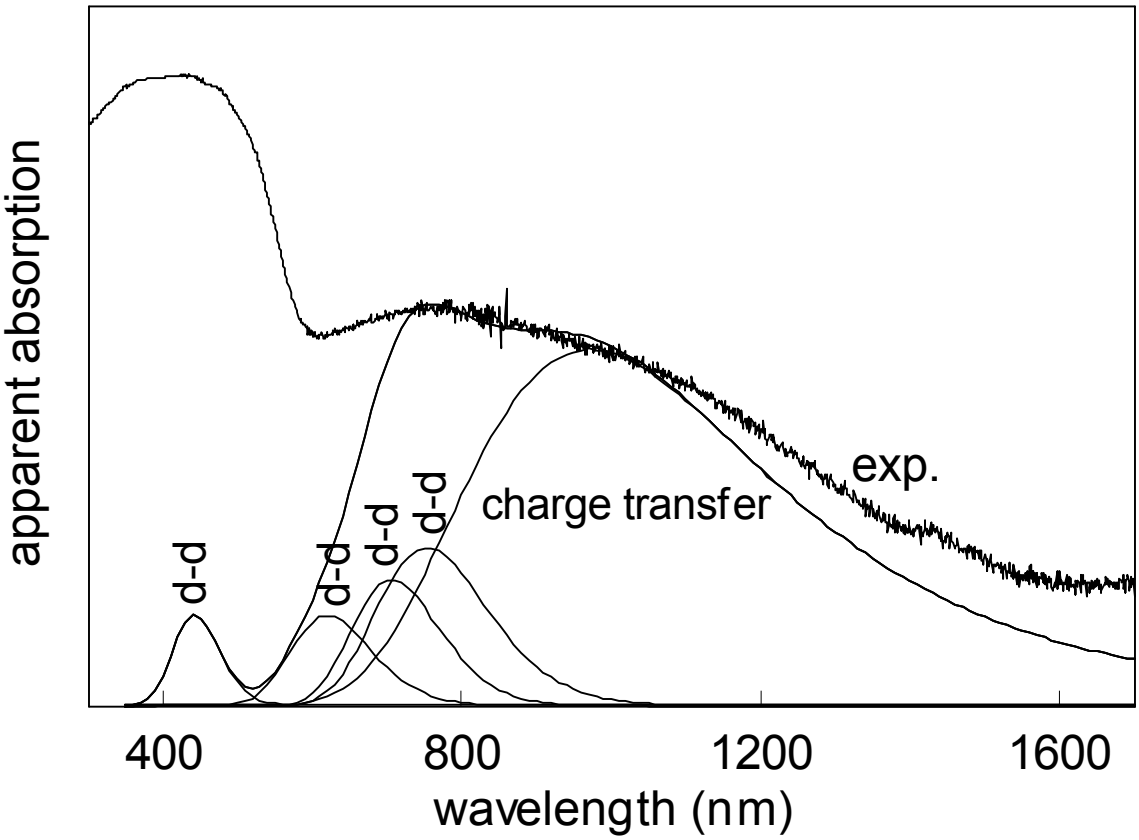
apparent absorption
d-d
d-d
d-d
d-d
charge transfer
exp.
400
800
1200
1600
wavelength (nm)

Figure 5

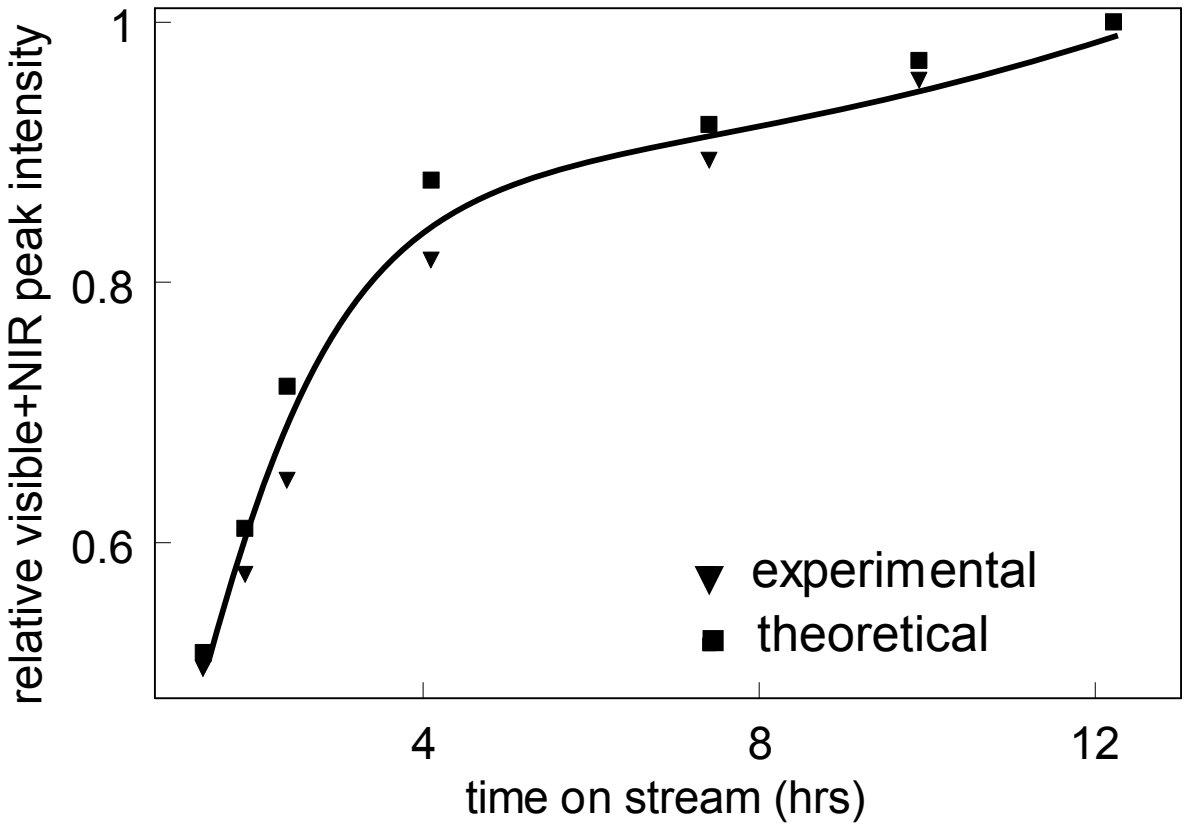
relative visible+NIR peak intensity
1
0.8
0.6
4
8
12
time on stream (hrs)
experimental
theoretical

Figure 6